Quantitative relations between cooperative motion, emergent elasticity, and free volume in model glass-forming polymer materials

Beatriz A. Pazmiño Betancourt[a,b,1], Paul Z. Hanakata[b,2], Francis W. Starr[b,1], and Jack F. Douglas[a,1]

[a]Materials Science and Engineering, National Institute of Standards and Technology, Gaithersburg, MD 20899; and [b]Department of Physics, Wesleyan University, Middletown, CT 06459

The study of glass formation is largely framed by semiempirical models that emphasize the importance of progressively growing cooperative motion accompanying the drop in fluid configurational entropy, emergent elasticity, or the vanishing of accessible free volume available for molecular motion in cooled liquids. We investigate the extent to which these descriptions are related through computations on a model coarse-grained polymer melt, with and without nanoparticle additives, and for supported polymer films with smooth or rough surfaces, allowing for substantial variation of the glass transition temperature and the fragility of glass formation. We find quantitative relations between emergent elasticity, the average local volume accessible for particle motion, and the growth of collective motion in cooled liquids. Surprisingly, we find that each of these models of glass formation can equally well describe the relaxation data for all of the systems that we simulate. In this way, we uncover some unity in our understanding of glass-forming materials from perspectives formerly considered as distinct.

glass formation | elasticity | cooperativity | free volume | strings

There are numerous theoretical approaches aiming to describe the universal liquid dynamics approaching the glass transition. One class of theories emphasizes the importance of the congested nature of the local atomic environment in cooled liquids, focusing on the amount of "free volume" available to facilitate molecular rearrangement (1). This free-volume approach is also linked to the more modern jamming model of glass formation (2). Older treatments of glass formation based on this perspective can be traced back to Batchinski (3), Doolittle (4), and Hildebrand (5) for small liquids, and to Williams and coworkers (6) and Duda and Vrentas (7, 8) for polymer materials. There is also more recent work based on the free-volume perspective, for example, positron lifetime measurements (9) that probe the cavity structure of glass-forming (GF) liquids. Debye–Waller measurements (9, 10), based on neutron, X-ray, or other scattering measurements, emphasize another type of free volume that is associated with the volume explored by particles as they rattle about their mean positions in a condensed material. This type of free-volume modeling has also been refined to take into account the shape of these "rattle" volumes (11, 12).

Another family of glass-formation models emphasizes the emergent elasticity in glassy materials (13). These approaches build on the idea that the solid-like nature of glasses is one of their most conspicuous, and perhaps defining, properties. Dyre (13) and Nemilov (14) have argued that the activation energy for transport should grow in proportion to the shear modulus. The models of Hall and Wolynes (15) and Leporini and coworkers (10, 16) can also be included in this class if the Debye–Waller factor is taken as a measure of local material stiffness.

Approaches emphasizing the underlying complex potential energy surface have also found considerable phenomenological success (17). The venerable Adam–Gibbs (AG) theory of glass formation (18), and the more recent random first-order

transition theory (19), emphasize the temperature dependence of the configurational entropy in cooled liquids and its relation to collective motion, although these theories do not explicitly define the form of the "cooperatively rearranging regions" (CRRs). This approach can be extended by identifying these CRRs with string-like clusters of cooperative particle exchange motion (20–22) and analytic calculation of the configurational entropy (23). In addition to these approaches to glass formation, the mode-coupling theory (24), and dynamic facilitation models (25) postulate a "dynamical" glass transition that is unrelated to any underlying thermodynamic transition.

The diverse range of models for glass formation reminds us of the story of the blind men and the elephant, where they grasp at the elephant and describe its attributes in terms of the different parts of which they have happened to take hold. In this respect, all these various approaches to understand glass formation may be "valid," but are simply focusing on different manifestations of a larger beast.

As a step toward bringing together some of these seemingly disparate ideas, the present paper explores the extent to which the thermodynamic perspectives of glass formation in terms of elasticity, collective motion, and vibrational free volume represent complementary perspectives of the same complex object, i.e., GF liquids. In particular, we consider the potential correspondence among perspectives through the direct computation

Significance

Diverse viewpoints have been developed to understand the scientifically fascinating and universal dynamics of glass-forming fluids. Currently, there are several prevailing models in the scientific literature based on seemingly different physical conceptions of glass formation, a fact that limits both theoretical and technological development in many scientific fields. We address this fundamental problem by simulating polymer glass-forming materials having a wide variation in the temperature dependence of structural relaxation ("fragility"), and we show by direct comparison that existing models equally describe our data, revealing deep relations between them. In this way, we achieve a greater theoretical unity of understanding glass-forming materials that should aid many applications in materials development and biology, the preservation and aesthetic properties of food, and medical science.

of the relationship between the structural relaxation time determined from the density correlations and molecular free volume, defined in terms of the Debye–Waller factor $\langle u^2 \rangle$ and the scale of collective motion, defined in terms of the size L of string-like molecular displacements. We find that all these approaches offer an accurate description of our relaxation time data for a model bulk polymer melt, polymer–nanoparticle composites, and supported polymer films—immediately implying quantitative relationships between the scale of collective motion, Debye–Waller factor, and emergent elasticity in cooled liquids. The differing models of GF liquids indeed involve different perspectives on essentially the same phenomenon. Several recent papers have sought to establish quantitative relations between emergent elasticity, free volume, and configurational entropy theories of glass formation, but with inconclusive results (26–28).

Results

Free-Volume Model of Relaxation. It has long been appreciated, both intuitively and theoretically, that the equilibrium and transport properties of fluids depend on the space available for molecular motion, but the lack of methods to accurately compute or measure free volume has limited the development of this perspective. Batchinski noticed that the viscosity of many simple fluids is nearly independent of temperature at constant volume at elevated temperatures (3), suggesting the applicability of a free-volume description of molecular transport in liquids. Hildebrand (5) and Hildebrand and Lamoreaux (29) developed Batchinski's phenomenological relation further by introducing a critical reference volume V_0 such that the fluid viscosity scales as the fractional volume $\eta \sim V_0/(V - V_0)$, and they showed the wide applicability of this relation to many fluids at elevated temperatures. Deviations from the Batchinski–Hildebrand expression are observed in fluids below their melting temperatures, and Doolittle introduced the modified expression (4)

$$\eta \sim \exp[V_0/(V - V_0)], \qquad [1]$$

which describes the viscosity of many liquids, ranging from polymer fluids (5) to hard spheres (30), over a wide temperature and concentration range approaching T_g. The success of the empirical Batchinski–Doolittle relation for η prompted theoretical efforts to quantify free volume and to rationalize Doolittle's observations. The free-volume model was also greatly influenced by Fox and Flory (31–33), who interpreted the Doolittle expression as implying that the glass transition corresponds to a vanishing of "sufficient" free volume for molecular movement and implying a physical interpretation of Doolittle's free-volume parameter, V_0.

The Batchinski–Doolittle relation (Eq. 1) also offers one possible explanation for the widely used, empirical Vogel–Fulcher–Tammann (VFT) relation. In particular, if the specific volume is reasonably taken to vary linearly with temperature in the range of glass formation, $(V - V_0) \propto (T - T_0)$, so then Eq. 1 becomes the VFT equation,

$$\eta = \eta_0 \exp[DT_0/(T - T_0)], \qquad [2]$$

where D is a dimensionless constant that quantifies the strength of the T dependence of η. The reciprocal of D offers one definition of the fragility of glass formation (34). The same expression is normally argued to apply to the diffusion coefficient, structural relaxation time τ, and other transport properties.

Fig. 1 shows the applicability of the VFT equation to all our simulation data for the relaxation time τ of the coherent intermediate scattering function (density–density correlations), including data for the pure polymer melt, polymer nanocomposites (35), and thin polymer films (36, 37). This description of our data is uniformly excellent from a numerical standpoint, but the free-
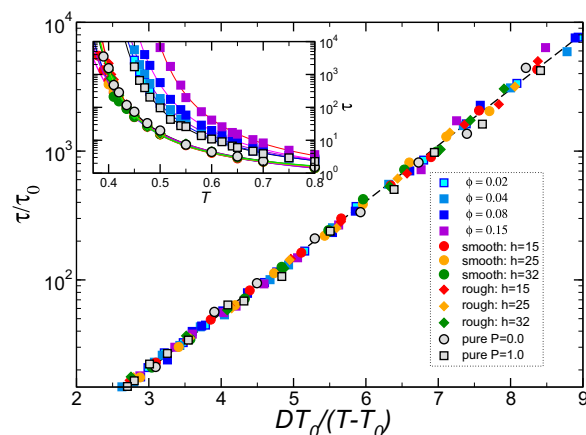
Fig. 1. VFT collapse of the temperature dependence of the relaxation time $\tau(T)$ for pure polymer melts, nanocomposites, and thin films. The triangles represent the pure melts at different pressures, $P = 0$ and $P = 1.0$, the squares represent the nanocomposite data, and the circles and diamonds represent the thin-film data for smooth or rough surfaces, respectively. For the nanocomposite data, the color gradient represents the increase in ϕ. (Inset) Temperature dependence of the segmental relaxation time $\tau(T)$, where the symbols represent the simulation data and the solid lines represent the VFT fits.

volume model provides little insight into the magnitude of η_0, D, and T_0, so that it is hard to predict trends with molecular structure.

Emergent Elasticity and Relaxation. To address questions relating to elasticity and relaxation, we first must identify an appropriate and physically accessible measure of material "stiffness." Both experiments and simulations have recently emphasized that the Debye–Waller factor $\langle u^2 \rangle$ also provides a useful measure of material stiffness. We can understand the physical grounds for this relation from the fact that the high-frequency plateau shear modulus G_p can be directly related to $\langle u^2 \rangle$, $G_p = 4k_BT/\pi\sigma\langle u^2 \rangle$ through a Langevin model for the Brownian motion, with a Maxwell model of viscoelasticity incorporated to describe transient caging (23). Recent simulations of a coarse-grained polymer melt, similar to the model described in the present paper, found good conformity with this relation (38). The Debye–Waller factor $\langle u^2 \rangle$ measures monomer displacements on a time scale over which the particles are caged by their neighbors, and is thus accessible from both X-ray and neutron scattering measurements (39). Because $\langle u^2 \rangle$ is usually determined experimentally at a fixed instrumental time, corresponding to the time scale on the order of vibrational motion of the molecules, we determine the mean-squared chain segment displacement at a caging time on the order of 1 ps.

We next explore the quantitative relation between τ and $\langle u^2 \rangle$. Based on the arguments and findings put forth by Hall and Wolynes (15) and Buchenau and Zorn (40), there should be a roughly linear scaling relation between $\log \tau$ and $1/\langle u^2 \rangle$. However, subsequent analyses for a range of systems have shown that such a relation exhibits systematic curvature (10–12, 16). Under the assumption that $\langle u^2 \rangle$ is a direct measure of free volume, simply requiring units of volume from $\langle u^2 \rangle$ in the Doolittle relation (Eq. 1) suggests a proportionality of $\log \tau$ with $\langle u^2 \rangle^{3/2}$, a relation we consider below based on more fundamental reasoning.

The localization model of relaxation (12) also starts from a free-volume perspective for relating τ and $\langle u^2 \rangle$. In particular, Simmons et al. (12) emphasize the anisotropic nature of the local free volume, and they propose the relation

$$\tau(\langle u^2 \rangle) = \tau_u \exp\left[(u_0^2/\langle u^2 \rangle)^{\alpha/2}\right], \qquad [3]$$

where τ_u is a constant prefactor, α is a measure of free-volume anisotropy, and u_0^2 is interpreted as a critical particle oscillation distance required for a particle to escape its "cage." As indicated above, one would expect $\alpha = 3$ for roughly spherical volumes on dimensional consistency grounds. The scaling of the volume with $\langle u^2 \rangle$ for volumes that are highly anisotropic should lead to variation of α. Simmons et al. treated the parameters τ_u, u_0^2, and α as fit parameters (12), and our data can be well described by Eq. 3, where these parameters are allowed to vary freely. Similarly, the model of Leporini and coworkers (10, 16) fits just as well if the same number of parameters is allowed to vary, so it is clearly desirable to reduce the number of free parameters to better understand their physical origin and have a more predictive relationship.

To do so, we take the localization model (Eq. 3) further by defining the parameters τ_u and u_0^2 through direct observation, rather than treating them as fit parameters. Specifically, we consider the fluid properties at the onset temperature T_A for dynamics influenced by glass formation. In particular, T_A marks the temperature where particle caging first emerges, and non-Arrhenius $\tau(T)$ dependence becomes apparent; its determination is briefly discussed in *Materials and Methods*. Accordingly, $u_A^2 \equiv \langle u^2(T_A) \rangle$ defines a natural reference scale of localization and $\tau_A \equiv \tau(T_A)$ defines the corresponding time scale. If we choose $u_0^2 \equiv u_A^2$, then consistency of Eq. 3 requires that $\tau_u = e\tau_A$ (where e is Euler's constant). With these definitions, Eq. 3 becomes

$$\tau(\langle u^2 \rangle) = \tau_A \exp\left[(u_A^2/\langle u^2 \rangle)^{\alpha/2} - 1\right], \qquad [4]$$

leaving only one free parameter, α, because τ_A and u_A^2 are obtained directly from our simulation data. For the specific case of isotropic free-volume equals, the localization model anticipates $\alpha = 3$ (12). Thus, in the spherical cage approximation, there are no free parameters in this revised localization model.

We now test the validity of Eq. 4 to quantitatively describe our simulation results. Fig. 2 shows the scaled relaxation data τ/τ_A as a function of scaled Debye–Waller factor $u_A^2/\langle u^2 \rangle$ for nanocomposites and thin-film systems, and the dashed lines indicate the fits to Eq. 4. For both cases, nanocomposites and thin films, the data nearly collapse to a master curve, described by Eq. 4 where $\alpha \approx 3.11 \pm 0.07$ for nanocomposites and $\alpha \approx 3.45 \pm 0.15$ for thin films. In *SI Text*, we also consider fixing $\alpha = 3$. The average value of τ_A for the entire set of GF liquids that we study is in the range $\tau_A = 4.1 \pm 0.4$, the average value of u_A^2 for thin films is $u_A^2 = 0.127 \pm 0.003$, and for nanocomposites it is $u_A^2 = 0.154 \pm 0.007$. In Fig. 3, we show the variation of these values for all systems considered. In physical units, τ_A is on the order of 1 ps for all systems investigated. This modified version of the localization model (12) of GF liquids provides a systematic way of obtaining the parameters of the model.

Cooperative Motion and Relaxation. AG (18) proposed an intuitively appealing and enduring conceptual picture for relaxation in GF liquids in which the activation free-energy barrier for molecular relaxation is assumed to increase in proportion to the number particles involved in hypothetical CRRs. The random first-order transition (RFOT) theory of Lubchenko and Wolynes (19) is related to the AG theory, in the sense that it also postulates dynamic CRR clusters ("entropic droplets") whose geometrical size (rather than the number of particles) determines the activation barrier for relaxation. The conception of such dynamic clusters has framed many modern investigations of dynamical heterogeneity in GF fluids, but, unfortunately, neither the AG nor RFOT theories offers a prescription for defining the CRRs. Simulation has led the way in defining the existence and
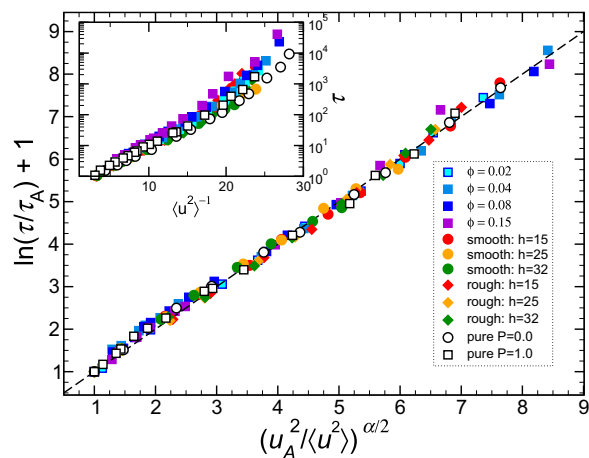

Fig. 2. Collapsed data of the relative $\tau/\tau_A + 1$ vs. $(u_A^2/\langle u^2 \rangle)^{\alpha/2}$. The data include the pure polymer melts at constant pressure $P = 0$ and $P = 1$, thin films with rough and smooth surfaces, and attractive NP nanocomposite systems. The symbols represent the simulated data points and the dashed line represent their linear relationship. (*Inset*) Variation of τ vs. $\langle u^2 \rangle$.

precise nature of cooperative motion in cooled liquids. In particular, several studies have established that the activation free-energy barrier ΔG for structural relaxation is proportional to the average length of string-like clusters involving particle exchange motion (20, 21, 34–37, 41). These well-defined string clusters provide a concrete realization of the CRRs. Notably, these "strings" have been observed for all of the systems we examine here, as well as in other materials, ranging from the grain boundaries of crystals and the interfacial dynamics of nanoparticles (42–44), to driven granular systems (45) to lipid membranes (46). The ubiquity of the phenomenon suggests that the dynamics of dense, strongly interacting particle systems may be generally characterized by string-like collective motion. Another aspect of the AG approach that has become apparent from recent molecular simulation is the importance of including the entropy of activation in the free energy of activation (21, 35, 37); AG made the unwarranted assumption that this quantity could be neglected. The approach of AG is further advanced by recognition that the strings can be analytically described as a kind of equilibrium polymerization, enabling a functional form for string length L that can be extended to the glass transition (21). Recently, Freed (22) provided an analytic extension of transition state theory that accounts for string-like cooperative barrier crossing events, providing a theoretical basis for the string model extension of the AG description (21). Our analysis of data starts from this fully developed "string model" of relaxation, a quantitative descendant of the AG model that preserves the original AG conception of the physical nature of glass formation.

The central prediction of the string model of glass formation is that the activation free energy for structural relaxation is proportional to the average string length L, where the proportionality factor is unity at T_A, i.e., $\Delta G = \Delta\mu(L/L_A)$, so that

$$\tau(T) = \tau_0 \exp[\Delta\mu(L/L_A)/k_B T], \qquad [5]$$

where $\Delta\mu$ is the activation free energy, $\Delta\mu(T) = \Delta H - T\Delta S$ at high temperatures, i.e., $T > T_A$, $L_A \equiv L(T_A)$, ΔH and ΔS denote the enthalpy and entropy of activation, respectively, and τ_0 is an (inverse) vibrational attempt frequency. As noted before, AG neglected the entropic contribution ΔS to the free energy of activation, and we shall see that this term plays a significant role in describing the dynamics of polymer films and nanocomposites.

Similar to our approach to reduce the number of free parameters in the localization model, we can reduce the number of

Fig. 3. Characteristic time τ_A and localization scale u_A^2 extracted from simulations data for the film (*Left*) and composite systems (*Right*) at the onset temperature T_A. For films, parameters are shown as a function of inverse thickness h_g^{-1} at T_g, and for composites as a function of nanoparticle concentration ϕ. (*Bottom*) Values of α from the best fit to Eq. **4**. Note that the variations of τ_A, u_A^2, and α are all small.

adjustable parameters in Eq. **5** through the introduction of the reference values $\tau(T_A)$ and $\Delta\mu_A = \Delta\mu(T_A)$. Demanding consistency with Eq. **5** then implies,

$$\tau(T) = \tau_A \exp[\Delta\mu(T)(L/L_A)/k_B T - \Delta\mu_A/k_B T_A]. \quad [6]$$

Because τ_A and L_A are taken directly from the simulated data, the activation free-energy parameters ΔH and ΔS are the only parameters adjusted in Eq. **6**. Conveniently, these basic transition state theory parameters can be determined by simulations at high T, and have a definite physical meaning in transition state theory.

We test the validity of Eq. **6** to quantitatively describe our simulation results in Fig. **4**, which show a remarkable collapse of all data, supporting the validity of this approach. Fig. 4 (*Insets*) shows that the activation parameters exhibit a linear entropy–enthalpy "compensation" relation, a phenomenon commonly observed in the dynamics and thermodynamics of condensed materials (47–49). Obviously, such a compensation relation cannot be recognized if ΔS is neglected, as in the original AG formulation. It is not common for the enthalpy of activation to become negative. This unusual type of kinetics has been observed in materials characterized by complex energy landscapes (50–53), and negative activation parameters are observed in zeolite materials where confinement is very strong (54, 55). The enthalpy–entropy compensation temperature, T_{comp} (the slope of the linear relation) for the nanocomposites and thin films, is close to the estimated VFT temperature T_0 of their pure systems, as found in previous experimental studies of β-relaxation in GF liquids (56–58). Our data reduction in terms of

the scale of collective motion is equally as compelling as the relation indicated above between τ and $\langle u^2 \rangle$.

By extension, consistency between these relations for τ implies a direct and precise relation between $\langle u^2 \rangle$ and the scale of string-like collective motion, L, so that

$$\frac{\langle u_A^2 \rangle}{\langle u^2 \rangle} = \left(\frac{L(T)}{L_A} \frac{\Delta\mu}{k_B T} - \frac{\Delta\mu_A}{k_B T_A} + 1 \right)^{2/\alpha}. \quad [7]$$

We test this relationship for the nanocomposite and thin-film systems. Fig. 5 illustrates the relationship between the scale of collective motion and the Debye–Waller factor (Eq. **7**) for $T < T_A$. This relation, together with the characterization of the string-like collective motion, allows us to understand how the cooperative motion of particles influences $\langle u^2 \rangle$. Moreover, we have recently developed and tested the validity of a polymerization model which predicts the T dependence of the extent of cooperative motion (21). Combining the present results with the theory of ref. 21, we can then predict the T dependence of $\langle u^2 \rangle$ in

Fig. 4. Test of the string model for cooperative relaxation $\ln(\tau/\tau_0)$ vs. $\Delta\mu(L/L_A)/k_B T$ for the thin films (*A*), and for the nanocomposite (*B*). The symbols represent the simulated data, and the dashed lines illustrate their linear relationship. (*Inset*) Enthalpy ΔH vs. entropy ΔS, parameters of the activation free energy $\Delta\mu$, in which, for both cases, they are linearly related with a characteristic temperature T_{comp}. For both cases, ΔH and ΔS are fit parameters of Eq. **6**, and τ_0 is not a free fitting parameter; it is determined by $\tau_0 = \tau_A \exp[-\Delta H/k_B T_A + \Delta S/k_B]$.

PHYSICS

Fig. 5. Relation between L and $\langle u^2 \rangle$ for all simulated data (nanocomposites and thin films). This figure shows the direct relationship (Eq. **7**) of the extent of cooperative motion L with $\langle u^2 \rangle$, an elastic property independently determined for all GF liquids simulated.

terms of the extent of the cooperative motion. The inverse scaling relating between L and the fluid configurational entropy s_c (20) means that Eq. **7** implies a curious relation between $\langle u^2 \rangle$ and s_c that remains to be explored.

Conclusions

We have examined well-defined experimental molecular-scale measures of material elasticity, free volume, and the scale of cooperative motion in a class of model polymeric GF liquids whose fragility is varied over a large range by varying the nanoparticle concentration or film thickness. This unified analysis reveals that the description of the structural relaxation time τ obtained from the coherent intermediate scattering function can be quantitatively described in terms of each of these perspectives of glass formation. We find that the introduction of mathematical consistency conditions and a definition of the scale of $\langle u^2 \rangle$ relative to its value at T_A into the localization model of glass formation leads to a relation between τ and $\langle u^2 \rangle$ with only one free parameter. In previous work, we were able to describe τ in terms of an apparently distinct relation involving the scale of collective motion L and the high-temperature Arrhenius activation parameters, ΔH and ΔS. The success in combining these two analyses of the relaxation data for our nanocomposite simulations implies a remarkable relation between the scale of the emergent collective motion in GF liquids, L, and a measure of the emergent elasticity of GF liquids, $\langle u^2 \rangle$. From a separate perspective, $\langle u^2 \rangle$ can be interpreted as a measure of local free volume (11). Evidently, the free volume, emergent elasticity, and cooperative motion models of glass formation, when defined in terms of well-defined measures of these physical characteristics of GF liquids, lead to largely equivalent mathematical descriptions of the temperature dependence of structural relaxation in

GF liquids. Previous researchers have indeed been grasping at different parts of this physical animal called a "glass."

Materials and Methods

Data Analysis. The structural relaxation time τ is obtained by evaluating the coherent intermediate scattering function, $F(q_0,\tau) \equiv 0.2$, where q_0 is the wave vector at which the first peak of the structure factor is located. The coherent $F(q,t)$ function captures correlations that are absent in its self (or incoherent) part, and so the coherent relaxation time is necessary larger than the self part. Additionally, the coherent relaxation time has a direct relation to the molecular structure through the de Gennes narrowing hypothesis, and can have different T dependence than the self part. However, we anticipate our results would not differ in a qualitative way if we used only the self part of the relaxation function for our analysis. The "onset" temperature T_A for dynamics associated with glass formation plays an important role in our analysis, and there are several ways to estimate T_A. One common procedure is to define T_A by the temperature at which $\tau(T)$ departs from Arrhenius behavior, $\tau = \tau_0 \exp[\Delta E/k_B T]$ (59, 60). A complementary approach is to identify the temperature below which particle caging first emerges. A quantitative method to locate the onset of caging is to find the temperature at which the logarithmic derivative of the mean square displacements $d \ln\langle r^2(t) \rangle / d \ln t$ develops a minimum, which is typically near 1 ps in molecular fluids (20, 21, 37). The onset of non-Arrhenius relaxation and caging is not a sharp transition, so we use both approaches, and find consistent estimates of T_A. Once T_A is defined, we are able to reduce the number of free parameters in Eqs. **4** and **5**, as described in the main text.

Computational Model. Our findings are based on equilibrium molecular dynamics simulations of a common "bead–spring" model for polymer chains. Previous studies (34–37, 61) have shown that we can introduce substantial changes to the polymer relaxation time and its T dependence by the addition of nanoparticles to form nanocomposites, or by confinement in supported thin films. Consequently, these systems offer us a way to systematically vary both T_g, fragility, and cooperative motion, enabling us to test the robustness of our approach. For the polymer composites, the polymers are modeled using a common bead–spring model (62) in which each chain consists of 20 monomers, where all monomers interact via a Lennard Jones (LJ) potential, and neighboring monomers of a chain interact via a finitely extensible nonlinear elastic (FENE) potential with parameters $k = 30\epsilon$ and $R_0 = 1.5\sigma$, where ε and σ are the energy and length parameters of the LJ potential, respectively. We use periodic boundary conditions so that we mimic a perfect cubic lattice of nanoparticles (NP) with a variable NP concentration that determines their separation and consider both attractive and nonattractive interactions between NP and the polymer matrix. We simulate a wide range of NP concentration for both systems, because the type of NP interaction and NP concentration alters differently T_g and fragility of GF liquids (35). For the NP, we use the model studied in ref. 61, in which the NP is built from a collection of LJ particles bonded to form a large icosahedron similar in shape to buckyballs and gold NP. In the case of polymer films, bonded monomers are connected by a harmonic spring potential, rather than the FENE bond potential (63). The difference in the polymer bonding potential is a technical rather than a substantive difference, because the FENE model tends to crystallize under confinement (37, 64). We consider both smooth and rough substrates for the films. For the perfectly smooth substrate, the interaction between a monomer and the substrate is given by a "9-3" LJ potential. To model the rough wall, we tether the wall atoms to the sites of triangular lattice with a harmonic potential. Details of these substrate interactions are given in ref. 37. All values are reported in reduced (LJ) units where monomer mass $m = \sigma = \epsilon = 1$.

1. Ferry JD (1980) *Viscoelastic Properties of Polymers* (Wiley, Hoboken, NJ).
2. Liu AJ, Nagel SR (2010) The jamming transition and the marginally jammed solid. *Annu Rev Condens Matter Phys* 1(3):347–369.
3. Batchinski AJ (1913) Untersuchungen über die innere Reibung der Flussigkeiten. *Z Phys Chem* 84:643–706.
4. Doolittle AK (1951) Studies in Newtonian flow. I. The dependence of the viscosity of liquids on temperature. *J Appl Phys* 22(8):1031–1035.
5. Hildebrand J (1977) *Viscosity and Diffusion* (Wiley, New York).
6. Ferry JD, Landel RF, Williams ML (1955) Extensions of the Rouse theory of viscoelastic properties to undiluted linear polymers. *J Appl Phys* 26(4):359–362.
7. Vrentas JS, Duda JL (1977) Diffusion in polymer-solvent systems. I. Reexamination of the free-volume theory. *J Polym Sci, Polym Phys Ed* 15(3):403–416.
8. Duda JL, Ni YC, Vrentas JS (1979) An equation relating self-diffusion and mutual diffusion coefficients in polymer-solvent systems. *Macromolecules* 12(3):459–462.
9. Ngai KL, Bao L-R, Yee AF, Soles CL (2001) Correlation of positron annihilation and other dynamic properties in small molecule glass-forming substances. *Phys Rev Lett* 87(21):215901.
10. Ottochian A, Leporini D (2011) Universal scaling between structural relaxation and caged dynamics in glass-forming systems: Free volume and time scales. *J Non-Cryst Solids* 357(2):298–301.
11. Starr FW, Sastry S, Douglas JF, Glotzer SC (2002) What do we learn from the local geometry of glass-forming liquids? *Phys Rev Lett* 89(12):125501.
12. Simmons DS, Cicerone MT, Zhong Q, Tyagi M, Douglas JF (2012) Generalized localization model of relaxation in glass-forming liquids. *Soft Matter* 8(45):11455–11461.
13. Dyre J (2006) The glass transition and elastic models of glass-forming liquids. *Rev Mod Phys* 78(3):953–972.
14. Nemilov S (2006) Interrelation between shear modulus and the molecular parameters of viscous flow for glass forming liquids. *J Non-Cryst Solids* 352(26-27):2715–2725.

15. Hall RW, Wolynes PG (1987) The aperiodic crystal picture and free energy barriers in glasses. *J Chem Phys* 86(5):2943–2948.
16. Larini L, Ottochian A, De Michele C, Leporini D (2007) Universal scaling between structural relaxation and vibrational dynamics in glass-forming liquids and polymers. *Nat Phys* 4(1):42–45.
17. Debenedetti PG, Stillinger FH (2001) Supercooled liquids and the glass transition. *Nature* 410(6825):259–267.
18. Adam G, Gibbs JH (1965) On the temperature dependence of cooperative relaxation properties in glass-forming liquids. *J Chem Phys* 43(1):139–146.
19. Lubchenko V, Wolynes PG (2007) Theory of structural glasses and supercooled liquids. *Annu Rev Phys Chem* 58:235–266.
20. Starr FW, Douglas JF, Sastry S (2013) The relationship of dynamical heterogeneity to the Adam-Gibbs and random first-order transition theories of glass formation. *J Chem Phys* 138(12):12A541.
21. Pazmiño Betancourt BA, Douglas JF, Starr FW (2014) String model for the dynamics of glass-forming liquids. *J Chem Phys* 140(20):204509.
22. Freed KF (2014) Communication: Towards first principles theory of relaxation in supercooled liquids formulated in terms of cooperative motion. *J Chem Phys* 141(14):141102.
23. Dudowicz J, Freed KF, Douglas JF (2008) Generalized entropy theory of polymer glass formation. *Adv Chem Phys* 137:125–222.
24. Götze W, Sjogren L (1988) Scaling properties in supercooled liquids near the glass transition. *J Phys C Solid State Phys* 21(18):3407–3421.
25. Hedges LO, Jack RL, Garrahan JP, Chandler D (2009) Dynamic order-disorder in atomistic models of structural glass formers. *Science* 323(5919):1309–1313.
26. Wyart M (2010) Correlations between vibrational entropy and dynamics in liquids. *Phys Rev Lett* 104(9):095901.
27. Sen S (2012) Entropic vs. elastic models of fragility of glass-forming liquids: Two sides of the same coin? *J Chem Phys* 137(16):164505.
28. Yan L, Düring G, Wyart M (2013) Why glass elasticity affects the thermodynamics and fragility of supercooled liquids. *Proc Natl Acad Sci USA* 110(16):6307–6312.
29. Hildebrand JH, Lamoreaux RH (1976) Viscosity of liquid metals: An interpretation. *Proc Natl Acad Sci USA* 73(4):988–989.
30. Woodcock L, Angell C (1981) Diffusivity of the hard-sphere model in the region of fluid metastability. *Phys Rev Lett* 47(16):1129–1132.
31. Fox TG, Flory PJ (1950) Second-order transition temperatures and related properties of polystyrene. I. Influence of molecular weight. *J Appl Phys* 21(6):581–591.
32. Fox TG, Jr, Flory PJ (1951) Further studies on the melt viscosity of polyisobutylene. *J Phys Colloid Chem* 55(2):221–234.
33. Fox TG, Flory PJ (1954) The glass temperature and related properties of polystyrene. Influence of molecular weight. *J Polym Sci, Polym Phys Ed* 14(75):315–319.
34. Starr FW, Douglas JF (2011) Modifying fragility and collective motion in polymer melts with nanoparticles. *Phys Rev Lett* 106(11):115702.
35. Betancourt BA, Douglas JF, Starr FW (2013) Fragility and cooperative motion in a glass-forming polymer-nanoparticle composite. *Soft Matter* 9(1):241–254.
36. Hanakata PZ, Douglas JF, Starr FW (2012) Local variation of fragility and glass transition temperature of ultra-thin supported polymer films. *J Chem Phys* 137(24):244901.
37. Hanakata PZ, Douglas JF, Starr FW (2014) Interfacial mobility scale determines the scale of collective motion and relaxation rate in polymer films. *Nat Commun* 5:4163.
38. Schnell B, Meyer H, Fond C, Wittmer JP, Baschnagel J (2011) Simulated glass-forming polymer melts: Glass transition temperature and elastic constants of the glassy state. *Eur Phys J E Soft Matter* 34(9):97.
39. Bellissent-Funel MC, Filabozzi A, Chen SH (1997) Measurement of coherent Debye-Waller factor in in vivo deuterated C-phycocyanin by inelastic neutron scattering. *Biophys J* 72(4):1792–1799.
40. Buchenau U, Zorn R (1992) A relation between fast and slow motions in glassy and liquid selenium. *Europhys Lett* 18(6):523–528.
41. Gebremichael Y, Vogel M, Bergroth MNJ, Starr FW, Glotzer SC (2005) Spatially heterogeneous dynamics and the Adam-Gibbs relation in the Dzugutov liquid. *J Phys Chem B* 109(31):15068–15079.
42. Zhang H, Srolovitz DJ, Douglas JF, Warren JA (2009) Grain boundaries exhibit the dynamics of glass-forming liquids. *Proc Natl Acad Sci USA* 106(19):7735–7740.
43. Zhang H, Kalvapalle P, Douglas JF (2010) String-like collective atomic motion in the interfacial dynamics of nanoparticles. *Soft Matter* 6(23):5944–5955.
44. Nagamanasa KH, Gokhale S, Ganapathy R, Sood AK (2011) Confined glassy dynamics at grain boundaries in colloidal crystals. *Proc Natl Acad Sci USA* 108(28):11323–11326.
45. Berardi CR, Barros K, Douglas JF, Losert W (2010) Direct observation of stringlike collective motion in a two-dimensional driven granular fluid. *Phys Rev E Stat Nonlin Soft Matter Phys* 81(4 Pt 1):041301.
46. Starr FW, Hartmann B, Douglas JF (2014) Dynamical clustering and a mechanism for raft-like structures in a model lipid membrane. *Soft Matter* 10(17):3036–3047.
47. Alberding N, et al. (1976) Dynamics of carbon monoxide binding to protoheme. *J Chem Phys* 65(11):4701–4711.
48. Liu L, Guo Q-X (2001) Isokinetic relationship, isoequilibrium relationship, and enthalpy-entropy compensation. *Chem Rev* 101(3):673–695.
49. Douglas JF, Dudowicz J, Freed KF (2009) Crowding induced self-assembly and enthalpy-entropy compensation. *Phys Rev Lett* 103(13):135701.
50. Moore WR (1965) Entropy of activation of viscous flow in dilute solutions of high polymers. *Nature* 206(4980):184.
51. Kuznetsov SV, Shen Y, Benight AS, Ansari A (2001) A semiflexible polymer model applied to loop formation in DNA hairpins. *Biophys J* 81(5):2864–2875.
52. Makarov DE, Keller CA, Plaxco KW, Metiu H (2002) How the folding rate constant of simple, single-domain proteins depends on the number of native contacts. *Proc Natl Acad Sci USA* 99(6):3535–3539.
53. Han X, Lee R, Chen T, Luo J, Lu Y, Huang K-W (2013) Kinetic evidence of an apparent negative activation enthalpy in an organocatalytic process. *Sci Rep* 3:2557.
54. Gounder R, Iglesia E (2012) The roles of entropy and enthalpy in stabilizing ion-pairs at transition states in zeolite acid catalysis. *Acc Chem Res* 45(2):229–238.
55. Artioli N, Lobo RF, Iglesia E (2013) Catalysis by confinement: Enthalpic stabilization of no oxidation transition states by micropororous and mesoporous siliceous materials. *J Phys Chem C* 117(40):20666–20674.
56. Dyre JC (1986) A phenomenological model for the Meyer-Neldel rule. *J Phys C Solid State Phys* 19(28):5655–5664.
57. Vainas B (1988) A kinetic compensation effect on a hierarchical tree. *J Phys C Solid State Phys* 21(11):L341–L343.
58. Psurek T, Soles CL, Page KA, Cicerone MT, Douglas JF (2008) Quantifying changes in the high-frequency dynamics of mixtures by dielectric spectroscopy. *J Phys Chem B* 112(50):15980–15990.
59. Douglas JF, Hubbard JB (1991) Semiempirical theory of relaxation: Concentrated polymer solution dynamics. *Macromolecules* 24(11):3163–3177.
60. Sastry S, Debenedetti PG, Stillinger FH (1998) Signatures of distinct dynamical regimes in the energy landscape of a glass-forming liquid. *Nature* 393(6685):554–557.
61. Starr FW, Schroder TB, Glotzer SC (2002) Molecular dynamics simulation of a polymer melt with a nanoscopic particle. *Macromolecules* 35(11):4481–4492.
62. Grest GS, Kremer K (1986) Molecular dynamics simulation for polymers in the presence of a heat bath. *Phys Rev A* 33(5):3628–3631.
63. Peter S, Meyer H, Baschnagel J (2006) Thickness-dependent reduction of the glass-transition temperature in thin polymer films with a free surface. *J Polym Sci, B, Polym Phys* 44(20):2951–2967.
64. Mackura ME, Simmons DS (2014) Enhancing heterogenous crystallization resistance in a bead-spring polymer model by modifying bond length. *J Polym Sci, B, Polym Phys* 52(2):134–140.

PHYSICS